Electronic Supplementary Information

Electroanalytical platform for nereistoxin-related insecticides detection based on DNA conformational switching and exonuclease III assisted target recycling

Shunbi Xie[a,*], Chunyan Tang[a], Huan Liu[a], Tian-e Zhang[a], Ying Tang[a,*], Liumei Teng[a], Jin Zhang[b]

a Chongqing Key Laboratory of Environmental Materials and Remediation Technologies, College of Chemistry & Environmental Engineering (Chongqing University of Arts and Sciences), Chongqing 402160, PR China

b Chongqing Vocational Institute of Engineering, Chongqing 402260, PR China

* Corresponding authors: Shunbi Xie, Ying Tang

E-mail addresses: xieshunbi@163.com, tangying2282@163.com

Tel.: +86-023-61162815

Experimental section

Chemicals

Propyl *p*-hydroxybenzoate (PPB), atrazine (ATZ), oxybenzone (OBZ), cartap, bensultap (BST) were purchased from Kelong Chemical Company (Chengdu, China). Methyl parathion (MP), dimethyl sulfoxide (DMSO), 6-mercapto-1-hexanol (MCH) hemin, tris(2-carboxyethyl) phosphine (TCEP) was purchase from Aladdin Industrial Corporation (Shanghai, China). All synthetic DNA sequences are shown in Table S1, and 4-(2-hydroxyethyl)-1-piperazine ethane sulfonic acid sodium salt (HEPES) were provided by Sangon Inc. (Shanghai, China). Ultrapure water (18.2 MΩ/cm) was used for all experiments. All other chemicals were of analytical grade and used as received.

20 mM Tris-HCl buffer solution (containing 20 mM Tris, 140 mM NaCl, 5 mM KCl, 1 mM $CaCl_2$, 1 mM $MgCl_2$, pH 7.4) was used to prepare the DNA solution. 20 mM HEPES buffer solution (containing 20 mM HEPES, 200 mM NaCl, 50 mM KCl and 1% DMSO) was used to prepare hemin stock solution. 20 mM phosphate buffer solution (PBS, pH 7.4) was prepared with 20 mM $Na_2HPO_4 \cdot 12H_2O$, 20 mM KH_2PO_4, 20 mM KCl and used as the supporting electrolyte.

Table S1 DNA sequences used in this work.

Primer Name	Sequence (5' to 3')
HP ssDNA with 2 C mismatch	ATCCACAGTAGTCCAT
HP ssDNA with 3 C mismatch	ATCCCACAGTAGTCCCAT
HP ssDNA with 4 C mismatch	ATCCCCACAGTAGTCCCCAT
HP ssDNA with 5 C mismatch	ATCCCCCACAGTAGTCCCCCAT
H1	NH_2-$(CH_2)_6$-TTT CAC AGT GGG CGG GAT GGG TGA ATG GGA CTA CTG TGG GAT

Apparatus and measurements

All electrochemical measurements, including cyclic voltammetry (CV), electrochemical impedance spectroscopy (EIS), differential pulse voltammetry (DPV), were conducted using CHI 660E electrochemical workstation (Shanghai Chenhua instrument, China) at room temperature with a conventional three-electrode system. A modified glassy carbon electrode (GCE, 4 mm in diameter) as the working electrode, platinum wire as the counter electrode, and saturated calomel electrode (SCE) as the reference electrode. The morphological characterization was performed with atomic force microscopy (AFM, Vecco, USA).

CV and EIS were selected to characterize the electrochemical properties of the modified electrode in 5 mL of 5 mM $[Fe(CN)_6]^{3-/4-}$ solution. CV was scanned from -0.2 to 0.6 V at a scan rate of 100 mV/s. EIS was performed at a scanning frequency from 0.1 Hz to 100 KHz with a 0.005 V modulation amplitude. DPV tested the electrode response performance in 5 mL of 20 mM PBS buffer with the following conditions: 0.05 V modulation amplitude, -0.6 to 0 V scan potential range, 0.05 s pulse width, 0.0025 s sample width.

Gel electrophoresis analysis

NRT induced DNA configuration transformation and Exo III assisted target cycling strategies were analyzed by 10% non-denaturation polyacrylamide gel (PAGE). All DNA samples were prepared at a concentration of 4 μM. 10 μL of each DNA sample was loaded into notches of freshly prepared gel and ran at 120 V for 100 min in 1×TBE buffer, and then stained with 4S Green for 30 min. Finally, the gel was imaged by Tanon 5200 Multi Chemiluminescent/Fluorescence Image System.

Results and discussion

AFM characterization of the sensing interface

Atomic force microscopy (AFM) is one of the most promising tools used for the investigation of surface morphology because of its high force sensitivity[1-2]. Thus, AFM was further employed to investigate the stepwise modification process of the sensing interface. Fig. S1 showed a significant change of the surface morphology after each modified step. Fig.S1A shows the image of Au modified electrode, which displayed spherical particles. After immobilization of H1 on the Au modified electrode, we can observe that the spherical surface has been covered and the film became rough, illustrating the immobilization of H1 on the surface of Au (Fig. S1B). After blocking the modified electrode with MCH, more rough films can be observed (Fig. S1C). Subsequent treatment of the modified electrode with the target conversion solutions in the presence of Exo III, the thickness and morphology of the films have changed obviously (Fig. S1D), which suggested that the digestion of Exo III toward H1/HP DNA duplex is executed successfully. when the modified electrode is further treated with K^+ and hemin, fine particle morphology can be observed due to the formation of hemin/G-quadruplex complexes (Fig. S1E). The AFM results also validated that the proposed electrochemical biosensor is successfully fabricated.

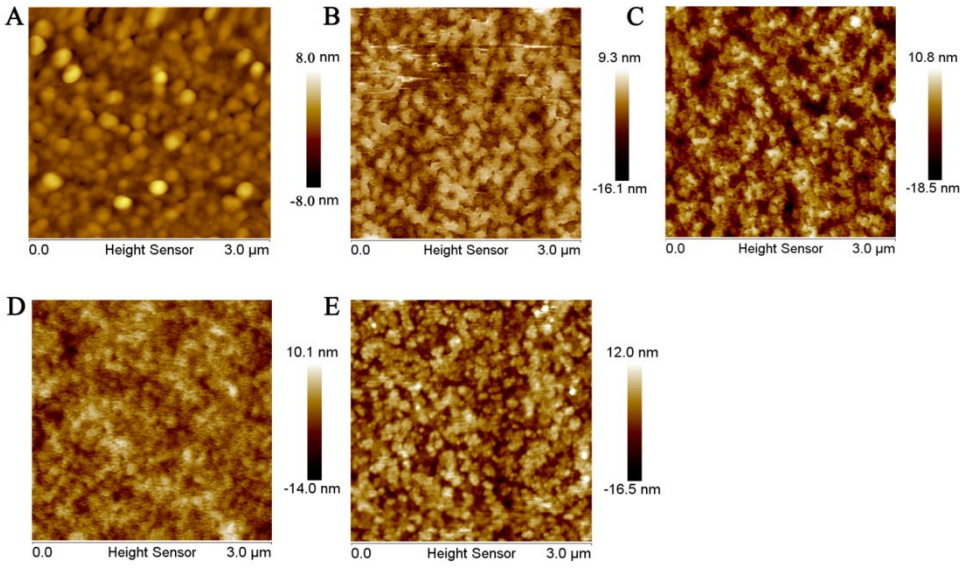

Fig. S1. AFM images of the modified films of: (A) electrode GCE/Au, (B) electrode GCE/Au/H1, (C) GCE/Au/H1/MCH, (D) electrode GCE/Au/G-quadruplex fragment/MCH, (E) electrode GCE/Au/hemin/G-quadruplex complexes/MCH.

The optimization of C-C mismatch numbers in HP ssDNA

Since this strategy is on the basis of HP ssDNA conformational switching triggered by Ag^+-removal, so the number of C-C mismatches in HP ssDNA is optimized to obtain the best signal-to-noise ratio. The number of C-C mismatches ranging from 2 to 5 in the stem were designed in HP ssDNA, and the electrochemical response of each HP ssDNA, in the absence (I (blank)) and presence of cartap (I (cartap)) were recorded, respectively. The DPV peak current changes ΔI ($\Delta I = I$ (cartap)-I (blank)) are shown in **Fig. S2**. From the results we can see that the 3 C-C mismatches in the stem of HP ssDNA give the most obvious electrochemical increment. This phenomenon can be explained by the following reasons: the HP ssDNA with 2 C-C mismatches possessing relatively high I (blank) owing to the weak stability of the HP ssDNA. Whereas, by increasing the number of C-C mismatches in HP ssDNA, more cartap is required to open the hairpin structured HP. And thus, under the same experimental conditions, the opened HP ssDNA is reduced and led to the formation of less G-quadruplex, which gave a relatively low I (cartap). The 3 C-C mismatches HP ssDNA possess the best signal-to-background ratio and therefore, is used in the detection system.

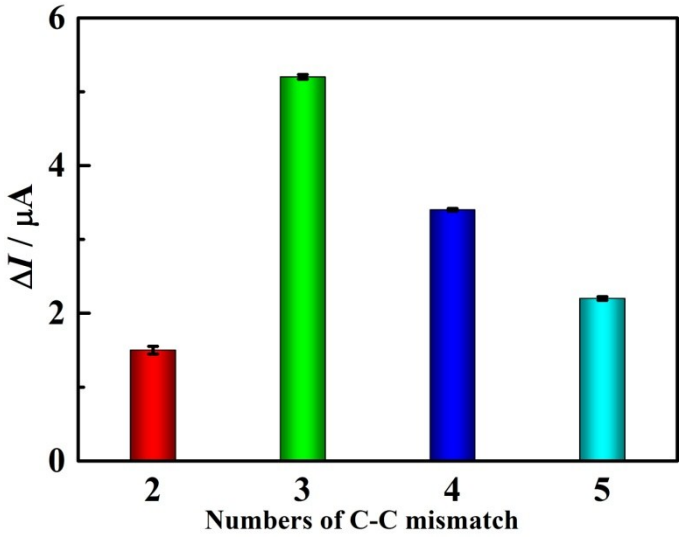

Fig. S2 Comparison of the DPV peak current change of the detection system by using HP with different numbers of C-C mismatch.

Table S2 Summary of different biosensors for NRT-related pesticides detection

NRT-related pesticides	Methods/Material	Linear range	Detection limit	Ref.
Cartap	Fluorescent/palmatine (PAL)-CB[7]	0.009-2.4 μg/mL	0.0029 μg/mL	3
Cartap	Fluorescent/AuNPs - CdTe QDs	0.01-0.50 mg/kg	8.24 mg/kg	4
Cartap	Fluorescent/carbon dots-AuNPs	5-300 nM	3.8 nM.	5
Cartap	Fluorescent/AuNPs - Rhodamine B	1-180 nM	0.88 nM	6
Cartap	Colorimetric/ Au NPs	0.05-0.6 mg/kg	0.04 mg/kg	7
Cartap	Colorimetric/ Au NPs	50-250 μg/kg	40 μg/kg	8
Cartap	Colorimetric/ AgNPs	0.036-0.36 μg/L	0.06 μg/L	9

NRT	Colorimetric/ AuNPs	12-140 ng/mL	12 ng/mL	10
Bensultap	Electrochemical	1-25 μg/mL	--	11
Cartap	Electrochemical	0.01-1500 μg/L	3.9 ng/L	This work

Gas chromatography/mass spectrometry (GC/MS), liquid chromatography/mass spectrometry (LC/MS)

Table S3. Determination of cartap in real agricultural products.

Samples	**Added amount / (μg/L)**	**Method (mean ±SD, μg/L) and recovery (%)[a]**		**Relative error of the results (%)**
		Our method	**GC-MS method**	
Cabbage	0	--	--	--
	10	8.25±3.47 (82.5)	8.97±5.31 (89.7)	-8.03
	100	89.3±3.12 (89.3)	94.6±4.37 (94.6)	-5.60
	500	517±4.23 (103.4)	493±5.12 (98.6)	4.87
Apple	0	--	--	--
	10	7.94±5.67 (79.4)	8.31±4.47 (83.1)	-4.45
	100	10.2±3.69 (102.0)	9.54±3.79 (95.4)	6.91
	500	429±6.23 (85.8)	437±4.16 (87.4)	-1.83

[a] Recovery % = calculated concentration (μg/L)/added concentration (μg/L) × 100 %

Reference

1. C. Greiner, J. R.Felts, Z. T. Dai, W. P. King and R. W. Carpick, *Nano Lett*., 2010, **10**, 4640-4645.
2. C. Lee, Q. Y. Li, W. Kalb, X. Z. Liu, H. Berger, R. W. Carpick and J. Hone, *Science*, 2010, **328**, 76-80.
3. X. Jing, L. M. Du, H. Wu, W. Y. Wu and Y. X. Chang, *J. Integr. Agr*., 2012, **11**, 1861-1870.
4. J. J. Guo, X. Liu, H. T. Gao, J. X. Bie, Y. Zhang, B. F. Liu and C. Y. Sun, *RSC Adv*., 2014, **4**, 27228-27235.
5. Y. X. Yang, J. Z. Hou, D. Q. Huo, X. F. Wang, J. W. Li, G. L. Xu, M. H. Bian, Q. He, C. J. Hou and M. Yang, *Microchim. Acta*, 2019, **186**, 259.
6. L. Dong, C. J. Hou, H. B. Fa, M. Yang, H. X. Wu, L. Zhang, D. Q. Huo, *J. Nanosci. Nanotechnol*., 2018, **18**, 2441-2449.
7. W. Liu, D. H. Zhang, Y. F. Tang, Y. S. Wang, F. Yan, Z. H. Li, J. L. Wang and H. S. Zhou, *Talanta*, 2012, **101**, 382-387.
8. W. Liu, D. H. Zhang, W. X. Zhu, S. K. Zhang, Y. S. Wang, S. X. Yu, T. Liu, X. Zhang, W. T. Zhang and J. L. Wang, *Microchim. Acta*., 2015, **182**, 401-408.
9. S. Rahim, S. Khalid, M. I. Bhanger, M. R. Shah and M. I. Malik, *Sens. Actuators B Chem*., 2018, **259**, 878-887
10. F. Takahashi, N. Yamamoto, M. Todoriki and J. Jin, *Talanta*, 2018, **188**, 651-657.
11. H. Shimada, S. Noguchi, M. Yamamoto, K. Nishiyama, Y. Kitamura, T. Ihara, *Anal. Chem*., 2017, **89**, 5742-5747.